Synthesis and Characterization of Polyacrylamide-Grafted Coconut Coir Pith Having Carboxylate Functional Group and Adsorption Ability for Heavy Metal Ions

T. S. Anirudhan, M. R. Unnithan, L. Divya, P. Senan

Department of Chemistry, University of Kerala, Kariavattom, Trivandrum 695 581, India

Received 18 January 2006; accepted 15 May 2006
DOI 10.1002/app.25002
Published online in Wiley InterScience (www.interscience.wiley.com).

ABSTRACT: The present investigation was undertaken to evaluate the effectiveness of a new adsorbent prepared from coconut coir pith (CP), a coir industry-based lignocellulosic residue in removing metal ions from aqueous solutions. The adsorbent (PGCP-COOH) having a carboxylate functional group at the chain end was prepared by grafting polyacrylamide onto CP using potassium peroxydisulphate as an initiator and in the presence of *N*,*N*′-methylenebisacrylamide as a crosslinking agent. The adsorbent was characterized by infrared (IR) spectroscopy, thermogravimetry (TG), X-ray diffraction (XRD) patterns, scanning electron microscopy (SEM), and potentiometric titration. The adsorbent exhibits very high adsorption potential for the removal of Pb(II), Hg(II), and Cd(II) ions from aqueous solutions. The optimum pH range for metal ion removal was found to be 6.0–8.0. The adsorption process follows a pseudo-second-order kinetic model. The adsorption capacities for Hg(II), Pb(II), and Cd(II) calculated using the Langmuir isotherm equation were 254.52, 189.49, and 63.72 mg g^{-1}, respectively. Adsorption isotherm experiments were also conducted for comparison with a commercial carboxylate form cation exchanger. Different industry wastewater samples were treated by the PGCP-COOH to demonstrate its efficiency in removing heavy metals from wastewater. The reusability of the PGCP-COOH was also demonstrated using 0.2*M* HCl. © 2007 Wiley Periodicals, Inc. J Appl Polym Sci 104: 3670–3681, 2007

Key words: adsorption kinetics; coir pith; pseudo-second-order; adsorption isotherm; thermodynamic parameters; desorption

INTRODUCTION

The ability of inexpensive naturally occurring lignocellulosic materials to remove heavy metals from aqueous solutions is well documented. Some of the lignocellulosic materials reported to effectively sequester heavy metals include sawdust,[1] moss peat,[2] bagasse flyash,[3] and tree fern.[4] These materials were found to have good adsorption capacity due to substances inherently associated with cellulose such as lignin, tannin, and pectin, which contain polyphenolic and aliphatic hydroxyl and carboxylic groups. Direct applications of these materials were found to be limited due to leaching of organics into the solutions. Chemical modifications such as esterification, graft copolymerization, crosslinking, and quaternization have been used to improve the physical and chemical properties of the lignocellulosic materials.[5–7] Chemical modification of lignocellulosic materials, followed by functionalization, is a promising technique to improve the sorption potential as well as to prevent the leaching of organics. Incorporation of different functional groups into lignocellulosic residues, such as bagasse flyash,[8] sawdust,[9] coconut husk,[10] orange residue,[11] and banana stem,[12] has already been reported.

Coconut coir pith (CP) is a widely available and abundant natural material, which basically contains cellulose and lignin. After the separation of fiber, from the coconut husk, the coir pith has no use and is discarded as waste in the agricultural sector. CP accounts for about 0.3–0.4 kg of the weight of an average coconut. India is the market leader in the production of coconut fruit, producing 7.5 millions tons of waste coir pith yearly.[13] Any attempt to reutilize the CP will be worthwhile. Earlier workers[14,15] have developed anion exchangers from CP for the removal of anionic contaminants from wastewaters. Recently Parab et al.[16] carried out an adsorption study on CP for the removal of uranium from aqueous solutions. In this work, a new adsorbent carrying carboxylate functional group was prepared by graft copolymerization of acrylamide (AAm) and *N*,*N*′-methylenebisacrylamide (MBA) onto CP and characterized by FT IR, X-ray diffraction (XRD), scanning electron microscopy (SEM), surface area analyzer, and thermogravimetry (TG)/DTG. This study was designed to assess the effectiveness of the adsorbent in the removal of Pb(II),

Correspondence to: T. S. Anirudhan (tsani@rediffmail.com).

Contract grant sponsor: Council of Scientific and Industrial Research, New Delhi.

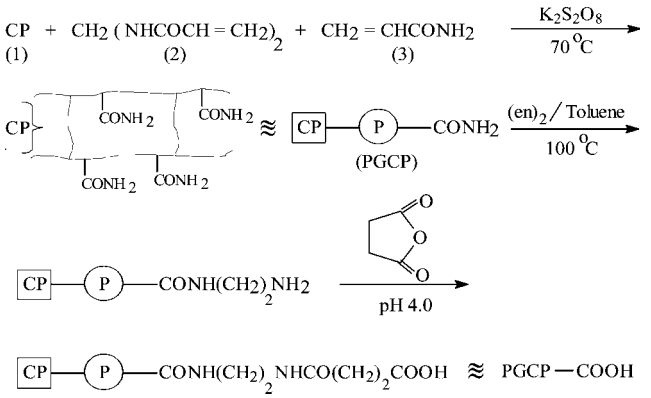

Scheme 1 Preparation of carboxylated polyacrylamide-grafted coconut coir pith.

Hg(II), and Cd(II) ions from aqueous solutions. To assess the practical utility of the adsorbent the recovery, regeneration, and comparison test application studies were also conducted. The results of the study are presented herein.

EXPERIMENTAL

Sorbent preparation

The CP collected from a local coir industry was washed several times with distilled water to remove dirt and water solubles and oven dried at 80°C for 24 h. The dried mass was sieved using standard test sieves to get particles of –80 to +230 mesh size. Scheme 1 represents the general procedure adopted for the preparation of poly(AAm)-grafted CP (PGCP) having —COOH group (PGCP-COOH). Twenty grams of CP (1) was immersed in 300 mL of an aqueous solution containing 5 g of MBA (2) as crosslinking agent and 2 g of potassium peroxydisulphate. Twenty five grams of AAm (3) was added to it and the mixture was stirred vigorously at 70°C in a water bath until a solid mass was obtained. The whole sample was extracted with water in a Soxhlet for 6 h in order to remove the homopolymer, poly-(AAm) formed during the grafting reaction, because the water can dissolve poly(AAm) easily. The PGCP obtained was washed with water and dried at 80°C. The control experiment was conducted in the same way as the graft for polymerization but in the absence of CP. The grafting parameters including the grafting percentage (GP) and grafting efficiency (GE) were determined as follows:

$$\mathrm{GP}\ (\%) = \left(W_p - W_o\right) \times 100/W_o \quad (1)$$

$$\mathrm{GE}\ (\%) = \left(W_p - W_o\right) \times 100/W_m \quad (2)$$

where W_o, W_p, and W_m are the weight of CP, purified graft copolymer, and AAm, respectively, determined gravimetrically.

The carboxylate functional group was incorporated into the matrix of the PGCP as follows. A certain amount of PGCP was refluxed with 25 mL ethylenediamine $(en)_2$ for 8 h. The product was separated and washed with toluene and dried. One part by weight of the above material (10 g) was refluxed at 90°C with an equal part by weight of succinic anhydride in 1,4-dioxane (100 mL) at constant pH 4.0 for about 6 h. The mixture was cooled and filtered, then washed with 1,4-dioxane. It was found that 3–5 times washing with 1,4-dioxane was quite enough to remove unreacted succinic anhydride. The product was washed with water and ethanol and finally air-dried. The PGCP-COOH obtained was sieved and particles having the average diameter 0.096 mm were used for adsorption experiments.

Equipment and methods of characterization

The FTIR spectra of CP and PGCP-COOH were taken in the range 400–4000 cm^{-1} on a Schimadzu FTIR model 1801. The samples were prepared as KBr pellets. The XRD patterns of the adsorbent samples were recorded using a Siemens D 5005 X-ray unit with Ni-filtered Cu Kα radiation. Thermal stability of the adsorbents was studied with a Metler Toledo Star thermogravimetric analyzer. A scanning electron microscope (Philips XL-30 CP) operated at 12 kV was used to probe the surface morphology of the adsorbents. The specific surface area of CP and PGCP-COOH was measured by BET N_2 adsorption using Quantasorb surface area analyzer (Qs/7). A potentiometric[17] method was used to determine the point of zero charge (pH_{pzc}). The cation exchange capacity (CEC) of the adsorbents was determined by $NaNO_3$ saturation method using a column operation. The apparent density of the adsorbents was determined by specific gravity bottle (10 mL capacity) using nitrobenzene as the displacing liquid. The concentrations of Pb(II), Hg(II), and Cd(II) ions in aqueous solutions were determined using a GBC Avanta A5450 atomic absorption spectrophotometer (AAS). A systronic microprocessor pH meter (model μ362, India) was used to measure the potential and pH of the suspension. For kinetic and isotherm studies a Labline (India) temperature controlled water-bath shaker (model L-12) with a temperature variation of ±1.0°C was used.

Adsorption and desorption experiments

The stock solutions of Pb(II), Hg(II), and Cd(II) ions (1000 mg L^{-1}) were prepared by dissolving $PbCl_2$, $HgCl_2$, and $CdCl_2$ (Fluka, Switzerland) in distilled water. Batch experiments were carried out in 100-mL stoppered conical flasks containing 50 mL solutions of different metal concentrations (25–750 mg L^{-1}) at pH 2.0–8.0 with 0.1 g of PGCP-COOH. The initial pH of

the solution was maintained by adding 0.1*M* HCl or NaOH using a pH meter. The flasks were shaken at an agitation speed of 200 rpm in a temperature-controlled water-bath shaker. At the end of predetermined time intervals, the sorbate was separated by centrifugation and the supernatant was analyzed for the residual metal concentration using AAS. The amount of metal adsorption was calculated based on the difference of metal concentration in aqueous phase before and after adsorption. The pH effect for metal adsorption was investigated in the pH range 2.0–8.0. Isotherm experiments were performed with varying concentrations of metals at a fixed adsorbent dose (2 g L^{-1}) at 30°C. Isotherm experiments were also conducted using a commercial cation exchanger Ceralite IRC-50 (CDH, Mumbai, India) without any pretreatment.

Desorption studies were carried out as follows: Initially the PGCP-COOH was loaded with metal ions by applying adsorption process for 3 h at pH 6.0. The metal-loaded adsorbent was agitated with 50 mL of 0.2*M* HCl for 3 h. Then the supernatant was centrifuged and analyzed for metals. The sorbent sample, thus, is regenerated and reused for adsorption purpose. Adsorption and desorption cycles were repeated four times. After each cycle, the sorbent was washed with distilled water and dried.

Statistical analysis

To ensure the accuracy, reliability, and reproducibility of the experimental data, all the batch experiments were performed in duplicate and the mean values were presented. In nearly all instances, the accuracy of data was very good, as the relative standard deviation was less than 3.0%. The kinetic and equilibrium parameters were obtained by a nonlinear optimization method using ORIGIN program (version 7.5). To quantitatively compare the fitness of kinetic and isotherm models the values of correlation coefficients (R^2) and chi-square (χ^2) were calculated.

RESULTS AND DISCUSSION

Graft copolymerization of AAm onto CP

The graft copolymerization reaction was monitored gravimetrically. The grafting of AAm onto CP, in the absence of MBA as crosslinking agent, leads to slightly soluble product in dilute acetic acid. This solubility characteristic together with the increase in weight of CP shows that the grafting has taken place effectively. When MBA was used as crosslinker, insoluble grafted CP, potentially useful as hydrogel, was obtained, which could be easily separated from the reaction medium and purified. The remarkable gain in the weight of residue, over the control reaction, gives a strong evidence for grafting of AAm onto CP. The values of GP and GE were determined and found to be 63 and 41%, respectively. Further evidence of the grafting was provided by the acid hydrolysis experiments. Fifty milligrams of PGCP was acid hydrolyzed by refluxing it with 1.0*M* HCl for 3 h. At the end of the reaction time, the content of the flask was poured into excess methanol. The product was filtered, washed several times with a methanol/water mixture (70:30, v/v), and dried. The residue was analyzed on a FT IR spectrophotometer. The infrared (IR) spectrum of the residue matched exactly with the IR spectrum of the hydrolyzed homopolymer, poly(AAm), giving further evidence of grafting AAm onto CP.

The mechanism of graft copolymerization of AAm onto lignocellulose has been studied extensively by earlier workers;[18,19] Shibi and Anirudhan[19] reported that lignin is more sensitive than cellulose to graft polymerization. Although the composition of lignocellulose and structure of lignin are rather complicated, the sensitive component for polymerization might be the phenolic hydroxyl groups of lignin. The grafting reaction initiated by potassium peroxydisulphate is characterized by first producing free radicals on the CP backbone and then adding AAm molecules to the CP macroradical formed ($CP^{\bullet}$). In the presence of AAm, CP is added to the double bond of AAm, resulting in a covalent bond between AAm and CP, with reaction of a free radical on the monomer, i.e., a chain is initiated. Thus, subsequent addition of AAm molecules to the imitated chain propagates the grafting reaction on to the CP as follows:

$$CP^{\bullet} + AAm \rightarrow CP - AAm^{\bullet} \quad (3)$$

$$CP - AAm^{\bullet} + AAm \rightarrow CP - (AAm)_2^{\bullet} \quad (4)$$

$$CP - (AAm)_{n-1}^{\bullet} + AAm \rightarrow CP - (AAm)_n^{\bullet} \quad (5)$$

Finally, the termination of the growing grafting chain may occur by coupling or combination, as follows:

$$CP - (AAm)_n^{\bullet} + CP - (AAm)_n^{\bullet} \rightarrow PGCP(\text{graft copolymer}) \quad (6)$$

Sorbent characterization

The possible assignments of the observed peaks in the FTIR spectra of CP and PGCP-COOH are furnished in Table I. The IR spectrum of CP shows an asymmetric absorption band at 3436 cm^{-1}, which is due to the hydrogen bonded O—H stretching vibration from the cellulose structure of the CP. The bands at 1782 and 584 cm^{-1} for CP arises due to the —C=O stretching of hemicellulose and β-glycosidic linkage.[12] The peak at 2928 cm^{-1} is indicative of the C—H stretching from the $—CH_2$ groups.

TABLE I
IR Spectroscopic Characteristics of CP and PGCP-COOH

Band (cm^{-1})	Assignment
CP	
3436	Sum of contributions of exchangeable O—H group (alcoholic and phenolic)
2923	C—H stretching vibrations of cellulose
2852	O—H stretching vibrations of H-bonding in cellulose
1614	Aromatic C=C stretching
1512	Aromatic C=C stretching
1462	CH_2 bending vibrations
1381	Aliphatic C—H bending
1271	C—O stretching
1051	C—O stretching
895	β-Glucosidic linkage
PGCP-COOH	
3530	Overlapped bands rising from ν_{N-H} of the amide group and ν_{O-H} of the carboxylic group along with O—H stretching band
2934	C—H stretching vibrations
2851	Intermolecular H-bonded O—H stretching
1762	Carbonyl C=O stretching
1629	Amide-carbonyl absorption band
1544	Amide group
1460	Carboxylic group
1384	Aliphatic C—H bending
1267	C—O stretching
1036	C—O stretching
608	Tortional vibration of pyranose ring

The IR spectrum of PGCP-COOH shows a broad peak centered at 3530 cm^{-1} and it is attributed to the overlapped band arising from ν_{N-H} of the amide group and ν_{O-H} of the —COOH group. The new peak at 1629 cm^{-1} indicates the existence of amide-carbonyl group on the grafted chain. The PGCP-COOH spectrum exhibits IR bands of carboxylate groups: due to stretching vibrations of C=O (at 1762 cm^{-1}), C—O (at 1267 cm^{-1}), and OH (at 3530 cm^{-1}). The raising in broad absorption band due to O—H stretching from 3436 cm^{-1} in CP to 3530 cm^{-1} in PGCP-COOH indicates the participation of OH group in the grafting of AAm on CP.

To determine the effect of poly(AAm) grafting of CP on thermal stability of the adsorbent, TG and DTG analyses were carried out. Figure 1 shows the TG and DTG curves of CP and PGCP-COOH. TG analysis reveals the intimate poly(AAm)-CP interaction gained through grafting, which causes the high thermal stability of PGCP-COOH with respect to CP. The values of the initial decomposition temperature (T_{Di}) were found to be 200 and 290°C for CP and PGCP-COOH, respectively. The weight loss of PGCP was relatively smaller than original CP. The temperature for 10% weight loss (T_{10}) is the basic criterion used to indicate the thermal stability of the polymers. The values of T_{10} were found to be 160°C for CP and 210°C for PGCP-COOH. DTG curves show that the decomposition of CP is produced in a single step with maximum temperature of weight loss at 336°C, whereas that in the PGCP-COOH decomposition appears at two decomposition maximas, the first one at 306°C and second one at 416°C. The Horowitz and Metzger[20] method was used to calculate E_a of the thermal degradation for CP and PGCP-COOH. Assuming that the order of reaction is unit, the following equation is used to calculate E_a values

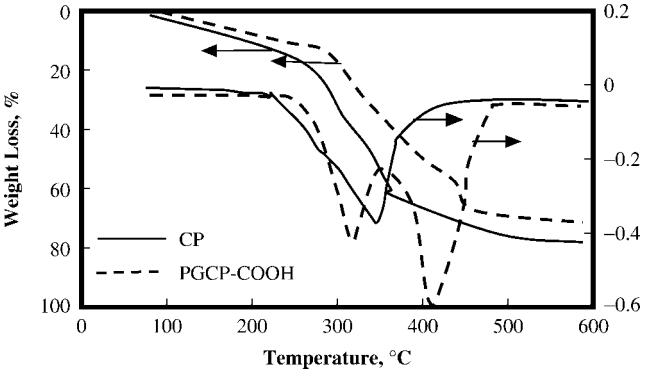

Figure 1 The TG and DTG curves of CP and PGCP-COOH.

$$\ln\left[\ln\left(\frac{w_o}{w_T}\right)\right] = \frac{E_a\theta}{RT_{max}^2} \quad (7)$$

where w_o is the initial weight of the material and w_T is the residual weight of polymer at temperature T, and θ is $T-T_{max}$. The E_a values were obtained from the slope of the plots of ln [ln (w_o/w_T)] versus θ (Fig. 2). The value of E_a of the thermal degradation for CP and PGCP-COOH were found to be 19.93 and 29.67 kJ mol^{-1}, respectively, indicating higher stability of PGCP-COOH.

The effect of graft copolymerization on the crystallinity of cellulose in CP was studied by XRD pattern. Structural changes of sorbents during chemical modi-

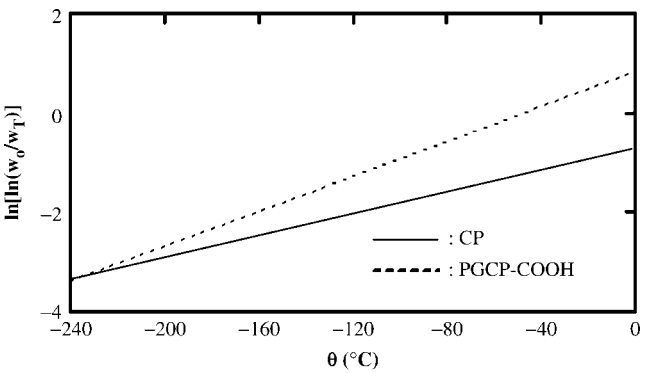

Figure 2 Plot of ln [ln (w_o/w_t)] versus θ for thermal degradation under nitrogen at a heating rate of 20°C min^{-1} of CP and PGCP-COOH.

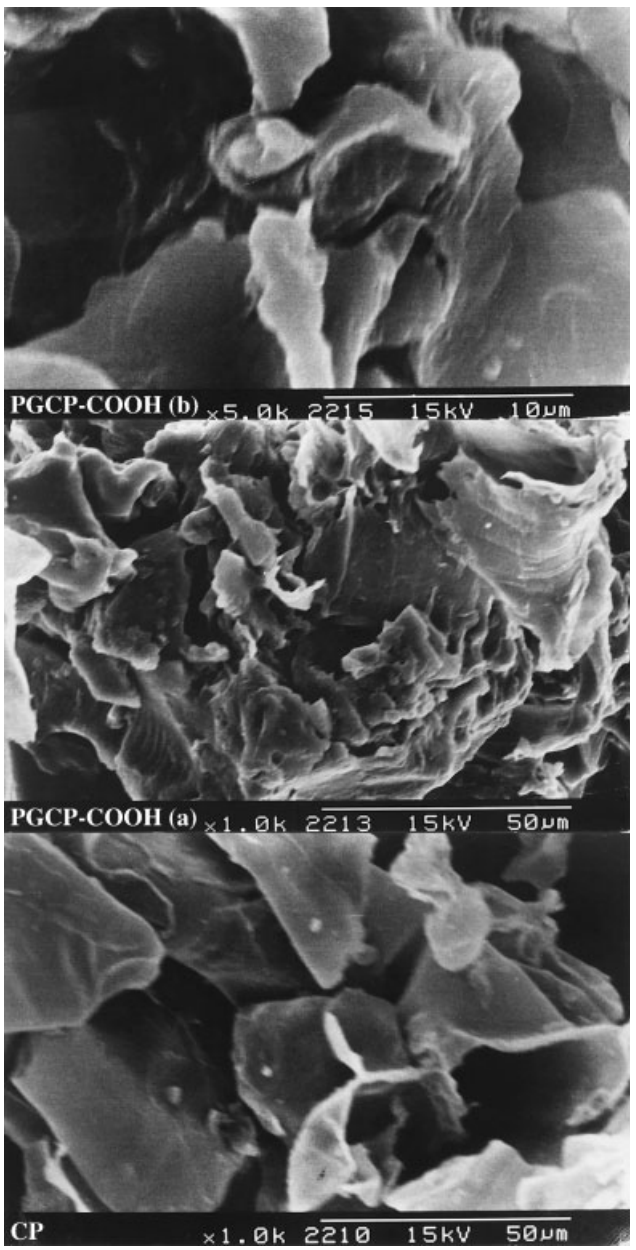

Figure 3 Scanning electron micrographs of CP and PGCP-COOH.

fication are very important for their adsorption capacity. The original CP shows scattering at $2\theta = 10.8^\circ$, 14.5°, 18.1°, and 34.3°, which are characteristic peaks of cellulose structure (figure not shown). The peak at $2\theta = 10.8^\circ$ due to the presence of (001) reflection and at $2\theta = 18.1^\circ$ due to the presence of (101) and (002) reflections indicating the presence of crystalline domains of cellulose structure[21] in CP. The absence of the peak at $2\theta = 10.8^\circ$ and 18.1° and the appearance of a broad peak at $2\theta = 22.2^\circ$ in PGCP-COOH indicate that the original CP lost its crystalline structure upon graft copolymerization reaction. The intensity and sharpness of the reflections decrease upon polymer grafting, confirming the decrease in crystallinity. It was thought that the decrease in crystallinity of PGCP-COOH was attributed to the deformation of the strong hydrogen bond in the original CP backbone where the hydroxyl groups were involved in grafting process.

Figure 3 shows the SEM micrographs of CP and PGCP-COOH. The SEM image of CP has unit cells that run longitudinally with parallel orientations and the intercellular voids can be clearly seen in CP. After 1.0 K × magnifications of SEM micrographs, PGCP-COOH shows the presence of folds on the surface, which resulted during the grafting of AAm. Some cracks and irregularities were also observed on the surface. Such cracks and irregularities are beneficial for the metal ions in the solution to diffuse to the inner adsorption sites located in the interior portion of the adsorbent. After 5.0 K × magnification, PGCP-COOH shows morphology of rough surface texture and porous structure. Like any polymer-grafted lignocellulosic material, PGCP-COOH is also hydrophobic in nature and its porous structure provides new adsorption sites from interior cavities to participate in binding of metal ions.

The surface charge density σ_o was determined by potentiometric method[17] using the following equation

$$\sigma_o = \frac{F(C_A - C_B) + [OH^-] - [H^+]}{A} \quad (8)$$

where F is the Faraday constant. A is the surface area of the suspension ($cm^2\ L^{-1}$), C_A and C_B are the concentrations of the acid and base (eq L^{-1}) after each addition during the titration and $[OH^-]$ and $[H^+]$ are the ions bound to the suspension surface (eq cm^{-2}). The value of pH_{pzc} obtained from the point of intersection of the σ_o versus pH plot (Fig. 4) was found to be 7.6 and 6.0 for CP and PGCP-COOH, respectively. The decrease of the pH_{pzc} after chemical modification indicates that the surface become more negative and this helps to bind positively charged metal cations. The

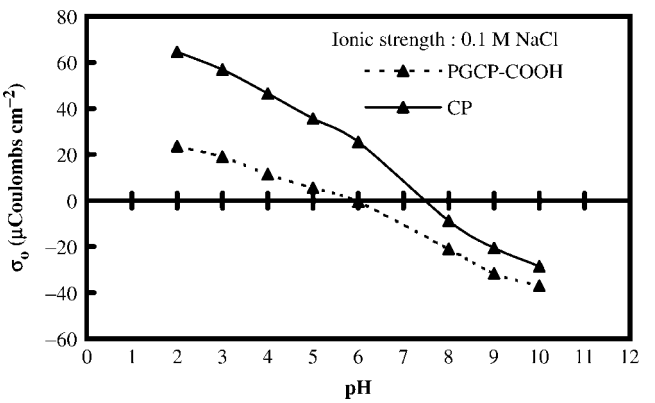

Figure 4 Surface charge density as a function of pH in aqueous solution of NaCl.

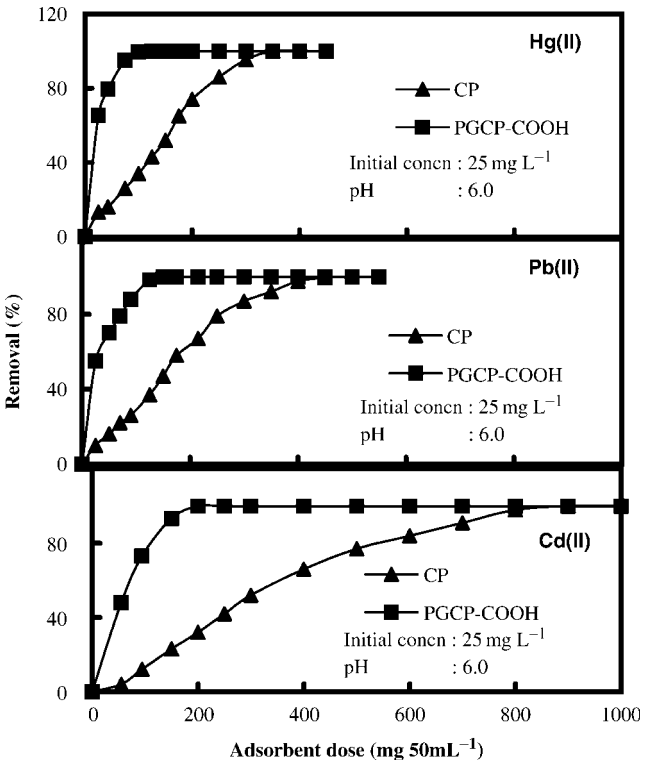

Figure 5 Effect of surface modification on metal adsorption.

surface area obtained from the N_2 adsorption isotherm was found to be 30.6 and 42.3 m^2 g^{-1} for CP and PGCP-COOH, respectively. The apparent density and CEC were found to be 0.82 g mL^{-1} and 0.39 meq g^{-1} for CP and 1.11 g mL^{-1} and 1.87 meq g^{-1} for PGCP-COOH, respectively.

Effect of surface modification on metal adsorption

The adsorption efficiency of CP and PGCP-COOH onto metal removal was examined by conducting batch experiments using an initial concentration of 25 mg L^{-1}, with varying adsorbent dose (Fig. 5). For the quantitative removal of 25 mg L^{-1} metal ions in 50 mL, a minimum adsorbent dosage of 125, 150, and 200 mg of PGCP-COOH and 350, 500, and 900 mg of CP was required for Hg(II), Pb(II), and Cd(II), respectively. The results clearly show that PGCP-COOH is 2.8, 3.3, and 4.5 times more effective than CP for the removal of Hg(II), Pb(II), and Cd(II), respectively. The higher metal removal obtained by PGCP-COOH may be explained by the increase in the adsorbent stability of the constituents present in CP, and thereby, the improvement in the access of metal ions to metal binding sites of the adsorbent. This is further confirmed by estimating the chemical oxygen demand (COD) in the solutions, which are treated with different amounts of CP and PGCP-COOH. When the adsorbent dose increased from 25 mg in 50 mL (0.5 g L^{-1}) to 450 mg in 50 mL (9 g L^{-1}), the values of COD increased from 33.2 to 316.7 mg L^{-1} in Hg(II) solution treated with CP, whereas for PGCP-COOH, the values increased from 6.3 to 30.6 mg L^{-1}. Chemical treatment induces stabilization of the hydrolysable compounds of CP by creating new bonds on constitutive units, and makes the CP able to adsorb metal ions without an increase in COD that is due to the release of phenolic compounds. Since PGCP-COOH had higher adsorption efficiency than CP, subsequent investigations on metal adsorption were made only with PGCP-COOH.

Effect of pH on metal adsorption

The effect of pH on metal adsorption onto PGCP-COOH was studied by changing the pH of the solution from 2.0 to 8.0 at an initial concentration of 25 mg L^{-1} and the results are shown in Figure 6. From this study it can be observed that the adsorption capacity of PGCP-COOH for metal removal increased with the increase of pH, but approached plateau value at the pH range 6.5–8.0 for Hg(II) and Pb(II) and 5.0–8.0 for Cd(II).The plateau values for metal ions at an initial concentration of 25 mg L^{-1} were found to be 12.48 mg g^{-1} (99.8%), 12.12 mg g^{-1} (97.6%), and 11.76 mg g^{-1} (94.1%) for Hg(II), Pb(II), and Cd(II), respectively. The final pH after adsorption was higher than the initial pH from 2.5 onwards. The adsorption of metal onto sorbent releases H^+ ions by ion exchange mechanism resulting in a decrease in solution pH at equilibrium. It should be noted that in the range of highest removal efficiency, the dominant metal species are M^{2+} and $M(OH)^+$ ions ($M \rightarrow$ Pb, Hg, Cd).[22] The removal of Pb(II), Hg(II), and Cd(II) by PGCP-COOH may be represented as

$$2\,\mathrm{PGCP-COOH} + \mathrm{M^{2+}} \rightleftharpoons (\mathrm{PGCP-COO})_2\mathrm{M} + 2\mathrm{H^+} \quad (9)$$

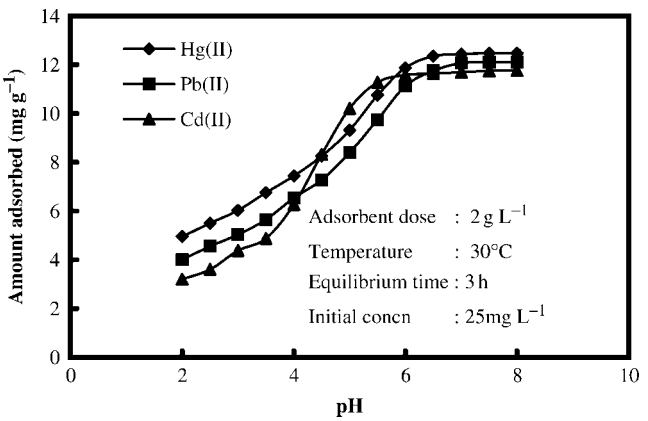

Figure 6 Effect of pH on the adsorption of metals on PGCP-COOH.

$$\text{PGCP} - \text{COOH} + \text{M(OH)}^{+} \rightleftharpoons \text{PGCP} - \text{COO}^{-}\text{MOH}^{+} + \text{H}^{+} \quad (10)$$

The pH_{pzc} of PGCP-COOH was found to be 6.0 and below this pH surface charge of the adsorbent is positive. The protonated effect on the carbonyl group increased with a decrease in the pH, and therefore the sites of negative charge of the PGCP-COOH are deficient in low pH. Therefore, at low pH values, the protonated surface because of the high H^+ ions concentration at the interface repels the positively charged metal ions electrostatically and prevents their approach to the PGCP-COOH surface. At pH greater than 6.0, PGCP-COOH becomes negatively charged and the metals, Pb, Hg, and Cd, were still present as $M(OH)^+$ species. Under this condition these metals were adsorbed through a favorable electrostatic attraction.

Effect of contact time and initial concentration

Experiments were performed to determine the time required for the metal removal process to reach equilibrium. The effects of contact time and initial metal concentration on the extent of removal are shown in Figure 7. From this study it can be observed that the amount of metals adsorbed increases with time and slowly reaches saturation within 3 h. The curve showed two distinct phases. The first phase involved rapid metal uptake in the beginning and 50–60% adsorption is completed within 15 min, followed by the subsequent removal of the metals, which continued for a longer period and attain saturation. The first phase may be attributed to the chemisorption type of interaction where as second phase indicates the utilization of all the active sites over the adsorbent surface and attainment of the saturation phase. The saturation time was found to be independent of initial concentration. By increasing the metal concentration from 25 to 100 mg L^{-1} at pH 6.0 the amount adsorbed increased from 12.48 mg g^{-1} (99.8%) to 60.03 mg g^{-1} (80.0%) for Hg(II), 12.11 mg g^{-1} (97.6%) to 55.13 mg g^{-1} (73.4%) for Pb(II), and 11.76 mg g^{-1} (94.1%) to 53.30 mg g^{-1} (71.1%) for Cd(II). These results clearly indicate that the removal of metal ions from aqueous solution is totally dependent on initial concentration. This is obvious because more efficient utilization of all the adsorption sites of the adsorbent is expected due to a greater driving force by a higher concentration gradient pressure. In all cases, the removal curves are single, smooth, and continuous, indicating the formation of monolayer coverage of metal ions on the surface of PGCP-COOH.

Kinetic modeling

The kinetics of adsorption is important from the point of view that it controls the process efficiency. Various

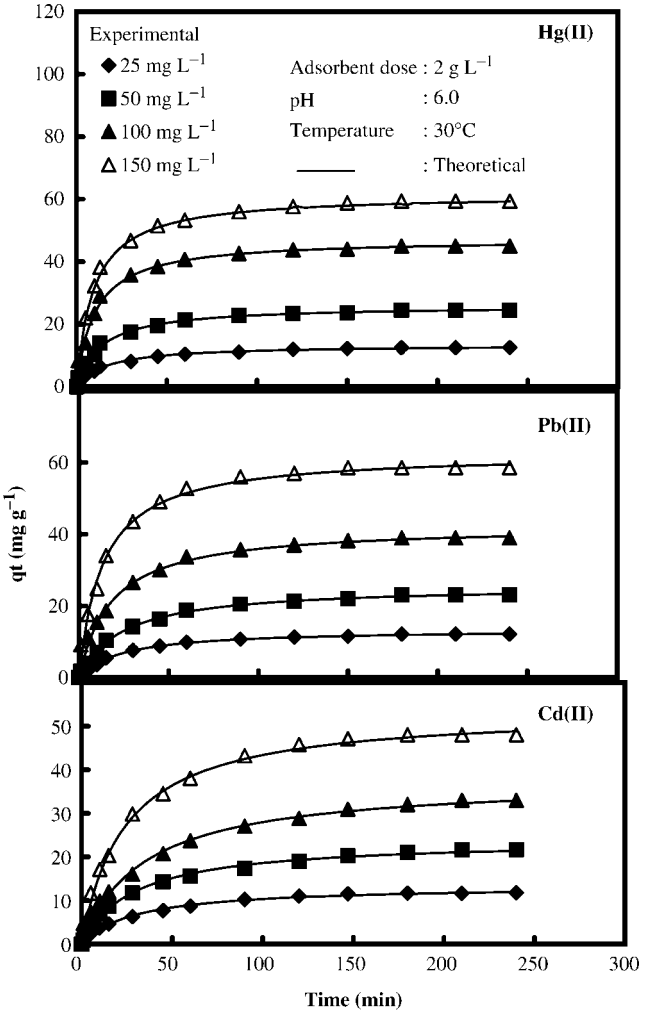

Figure 7 Typical plots of comparison between the experimental and pseudo-second-order modeled q_t versus time for the adsorption of metals onto PGCP-COOH for different concentrations.

models such as a first-order, psuedo-first-order, and Elovich equation have been used to describe the kinetics of adsorption. For many adsorption processes using heterogeneous materials, it was found that the pseudo-second-order kinetic equation agrees with chemisorption as the rate-controlling step.[23] Therefore a pseudo-second-order kinetic model as suggested by Ho and McKay[24] was used to describe all the kinetic data. The psuedo-second-order rate expression is defined by eq. (11) and the integrated form is given in eq. (12)

$$\frac{dq_t}{dt} = k(q_e - q_t)^2 \quad (11)$$

$$q_t = \frac{kq_e^2 t}{1 + kq_e t} \quad (12)$$

where k is the second-order rate constant (g mg^{-1} min^{-1}), q_e and q_t are the amount of metal ions

TABLE II
Pseudo-Second-Order Rate Constants for the Adsorption of Hg(II), Pb(II), and Cd(II) onto PGCP-COOH

	k (10^3 g mg^{-1} min^{-1})	q_e (calc)	R^2	χ^2
Concentration (mg L^{-1})				
Hg(II)				
25	4.53	13.34	0.997	0.214
50	2.79	26.01	0.996	0.080
100	2.06	47.28	0.997	0.214
150	1.72	61.57	0.998	0.360
Pb(II)				
25	3.13	13.43	0.998	0.045
50	2.60	25.70	0.998	0.141
100	1.92	42.43	0.995	0.106
150	1.21	62.73	0.999	0.236
Cd(II)				
25	2.48	13.43	0.995	0.084
50	1.43	23.97	0.996	0.251
100	0.89	37.59	0.997	0.233
150	0.77	53.65	0.998	0.202
Temperature (°C)				
Hg(II)				
30	2.06	47.28	0.997	0.214
40	2.52	48.55	0.997	0.180
50	2.84	50.89	0.998	0.412
60	3.71	51.44	0.999	0.106
Pb(II)				
30	1.92	42.43	0.995	0.106
40	2.31	44.86	0.999	0.361
50	2.74	48.33	0.999	0.404
60	3.60	51.20	0.999	0.188
Cd(II)				
30	0.89	37.59	0.997	0.233
40	1.65	40.32	0.997	0.126
50	2.50	42.60	0.999	0.321
60	3.01	47.14	0.999	0.256

adsorbed at equilibrium and at time t, respectively. The values of k and q_e for different concentrations and temperatures were calculated by a nonlinear optimization method using ORIGIN program (version 7.5) and the results are shown in Table II. To measure the degree of fitness of this model with actual kinetic data, correlation coefficients (R^2) and chi-square (χ^2) values were computed. Higher R^2 (>0.98) and lower χ^2 (<0.30) values obtained for pseudo-second-order model indicate that this model could define the experimental results in the present system. From Figures 7 and 8 it was observed that the theoretical values of q_t for all concentrations and temperatures were very close to the experimental q_t values. This suggests that the adsorption of metals follows the second-order kinetic model. The value of k decreases with an increase of initial concentration, whereas the value of q_e increases with the increase in initial concentration. The lower the concentration of metal ion in solution, the lower the probability of collisions between these ions, and hence the faster these metal ions could be bonded to the active sites on the adsorbent surface. From the table it can be shown that the values of k and q_e increased with increase of temperature. Since PGCP-COOH has relatively high q_e values, the adsorption rate became very fast and the equilibrium time is short. The short equilibrium time coupled with high adsorption capacity indicate a higher degree of affinity between the metals and the PGCP-COOH.[25]

The energetics of adsorption was also calculated from temperature studies. The values of activation energy (E_a) for the sorption reaction were determined using the Arrhenius equation. The rate constant k could be related to the temperature by the following relationship

$$\ln k = \ln k_o - \frac{E_a}{RT} \tag{13}$$

The E_a values were calculated from the slope of ln k versus $1/T$ plots (figure not shown) and the values were found to be 15.76, 17.19, and 34.57 kJ mol^{-1} for Hg(II), Pb(II), and Cd(II), respectively. Other kinetic parameters were calculated using the following Eyr-

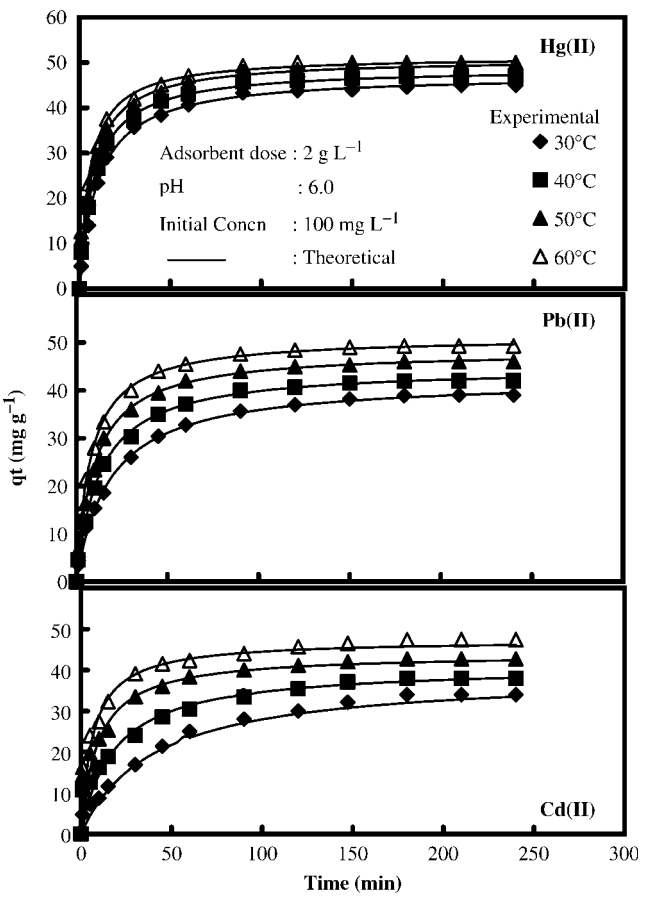

Figure 8 Typical plots of comparison between the experimental and pseudo-second-order modeled q_t versus time for the adsorption of metals onto PGCP-COOH for different temperatures.

ing equations[26]

$$\ln\frac{k}{T}=\left(\ln\frac{k_b}{h}+\frac{\Delta S^{\neq}}{R}\right)-\frac{\Delta H^{\neq}}{RT} \quad (14)$$

where k_b is the Boltzmann constant, h is Planck constant, T is the absolute temperature, $\Delta S^{\neq}$ is the entropy of activation, $\Delta H^{\neq}$ is the enthalpy of activation, and R is the gas constant. The plots of ln (k/T) versus $1/T$ for all metals were found to be linear (figure not shown). The values of $\Delta H^{\neq}$ and $\Delta S^{\neq}$ were obtained from the slope and intercepts of the plot. The free energy of activation $\Delta G^{\neq}$ can be calculated as $\Delta G^{\neq} = \Delta H^{\neq} - T\,\Delta S^{\neq}$. The values of $\Delta H^{\neq}$ and $\Delta S^{\neq}$ for the adsorption of metal ions were found to be 13.12 kJ mol^{-1} and –119.15 J mol^{-1} K^{-1} for Hg(II), 14.50 kJ mol^{-1} and –115.18 J mol^{-1} K^{-1} for Pb(II), and 31.71 kJ mol^{-1} and –63.94 J mol^{-1} K^{-1} for Cd(II), respectively. The positive values of $\Delta H^{\neq}$ suggest the endothermic nature of the process. The negative values of $\Delta S^{\neq}$ indicate a greater order of reaction during the adsorption of metal ions. The values of $\Delta G^{\neq}$ were found to be 49.23, 50.42, 51.61, and 52.80 kJ mol^{-1} for Hg(II), 49.43, 50.58, 51.73, and 52.89 kJ mol^{-1} for Pb(II), and 51.09, 51.73, 52.37, and 53.01 kJ mol^{-1} for Cd(II) at 30, 40, 50, and 60°C, respectively. The adsorption is endothermic; hence the amount adsorbed at equilibrium must increase with increase in temperature, because free energy of activation increases with the rise in temperature of a solution. This explains why the values of $\Delta G^{\neq}$ increase with rise in temperature.

Adsorption isotherm

The adsorption isotherms of metal ions from aqueous solution onto PGCP-COOH are plotted in Figure 9, expressed as the amount of metal ions adsorbed per gram of the adsorbent (q_e) versus the equilibrium concentration (C_e). It is obvious from Figure 9 that the adsorption isotherms of metals onto PGCP-COOH are L-type according to the Giles classification.[27] This indicates that all the adsorption sites are equivalent and that there is no interaction between adsorbed species. The initial curvature indicates that a large amount of metal ions is adsorbed at a lower concentration as more active sites of PGCP-COOH are available. As the concentration increases, it becomes difficult for a metal ion to find vacant sites, and so monolayer formation occurs. The most widely used isotherm equation for modeling the adsorption equilibrium is the Langmuir equation, which is valid for monolayer sorption onto a surface having finite number of identical sites and is expressed as

$$q_e=\frac{Q^0 bC_e}{1+bC_e} \quad (15)$$

where Q^o and b are the Langmuir constants related to adsorption capacity and energy of adsorption, respectively. C_e and q_e are the equilibrium metal concentration left in solution after adsorption (mg L^{-1}) and the amount of metal adsorbed to the adsorbent (mg g^{-1}), respectively. The values of Q^o and b were determined using nonlinear optimization method. The theoretical q_e values were very close to the experimental q_e values (Fig. 9). All the correlation coefficients obtained are more than 0.99.

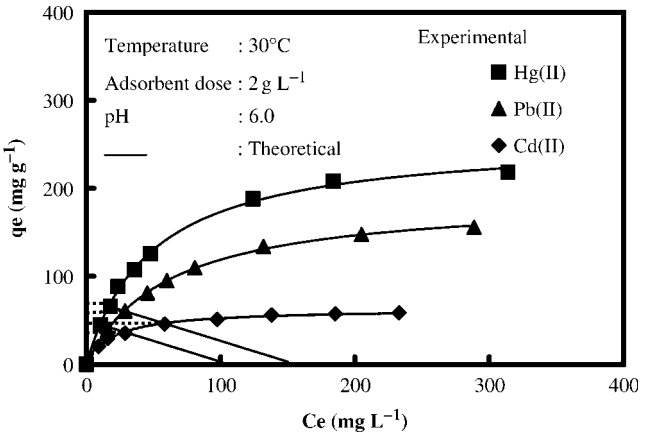

Figure 9 Experimental and calculated q_e versus C_e plots with the operating lines drawn for the adsorption of metals onto PGCP-COOH.

The values of Q^o and b at 30°C were found to be 254.52 mg g^{-1} and 0.021 L mg^{-1} for Hg(II), 189.49 mg g^{-1}and 0.016 L mg^{-1} for Pb(II), and 63.72 mg g^{-1} and 0.047 L mg^{-1} for Cd(II), respectively. The Q^o values for the adsorption of metal ions at 30°C by PGCP-COOH were compared with earlier reported literature data. The values of Q^o for adsorption of Hg(II) at 30°C by photo film waste sludge,[28] 2-mercaptobenzothiozole-treated clay,[29] 2-mercapto benzimidazole-treated clay,[30] and for commercial activated carbon[31] was found to be 11.76, 2.69, 102.49, and 12.38 mg g^{-1}, respectively. The values of Q^o at 30°C for Pb(II) adsorption were reported to be 58.89, 39.80, 31.05, and 2.37 mg g^{-1} for adsorption onto lignite,[32] tree fern,[33] montmorillonite,[34] and modified pyrophyllite,[35] respectively. Malakul et al.[36] have reported the Q^o values of 42.03 and 43.02 mg g^{-1} for adsorption of Cd(II) on surfactant-modified clay and Chelex-100 resin, respectively. The Q^o values for the adsorption of Cd(II) onto waste Fe(III)/Cr(III) hydroxide,[37] sawdust of *Pinus sylvestris*,[38] and ulva seaweed[39] were reported to be 40.49, 19.08, and 61.94 mg g^{-1}, respectively. These data clearly indicate that the adsorption capacity of PGCP-COOH is very much greater than the other adsorbents.

The operating line is the line that predicts the time dependence of a sorption process and integrates this dependence into the equilibrium isotherm. Consider V liters of solution and metal concentration is to be reduced from C_o to C_1 mg L^{-1}. The amount of sorbent

TABLE III
Comparison of the Equilibrium Sorption Capacity Evaluated from Langmuir Equation and the Pseudo-Second Order Model

	Concentration (mg L^{-1})	
Metals	100	150
Hg(II)		
q_e	47.28	61.57
q_{max}	46.90	62.42
Pb(II)		
q_e	42.43	62.73
q_{max}	42.10	62.60
Cd(II)		
q_e	37.59	53.65
q_{max}	37.95	54.21

m (gram) and the metal-loading changes from q_o to q_t and the mass balance equates the metal removal from the liquid to that sorbed by the adsorbent

$$(C_o - C_t)V = (q_t - q_o)m \tag{16}$$

If the system is allowed to come to equilibrium then

$$(C_o - C_t)V = (q_e - q_o)m \tag{17}$$

For fresh adsorbent, $q_o = 0$, it can be expressed as follows

$$q_e = -\frac{V}{m_s}C_e + \frac{V}{m_s}C_o \tag{18}$$

This material balance provides the operating line equation in Figure 9, using an initial concentration of 100 mg L^{-1}, adsorbent mass of 0.1 g and metal solution volume of 0.05 L. Figure 9 shows the operating lines, which are generated with a slope of solution volume per adsorbent mass (V/m). The final solution concentration is predicted from the point of intersection of operating line on the sorption isotherm. The equilibrium sorption capacity, q_m, can be obtained from the operating line and the Langmuir equation. The results are in reasonable agreement with the equilibrium sorption capacity, q_e, obtained from the pseudo-second-order model. A comparison is made between the equilibrium sorption capacity evaluated from Langmuir equation and the pseudo-second-order model in Table III, which shows the equilibrium sorption capacities evaluated are reasonable.

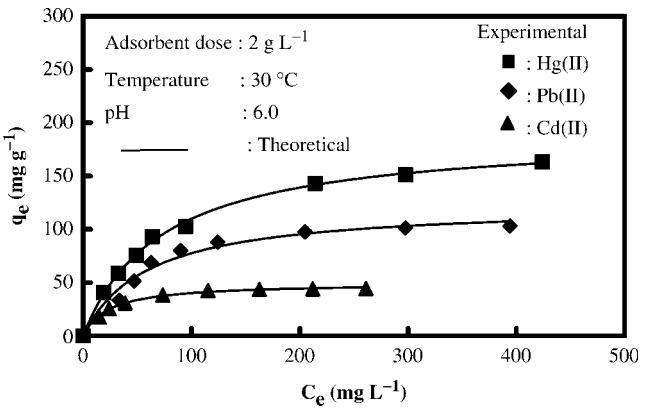

Figure 10 Adsorption isotherm plots for the adsorption of metals onto Ceralite IRC-50 at 30°C.

Comparison with commercial ion exchanger

Adsorption experiments were also performed using a carboxylate-functionalized commercial cation exchanger (Ceralite IRC-50) to compare the utility of the PGCP-COOH as an adsorbent. Adsorption data for Pb(II), Hg(II), and Cd(II) by Ceralite IRC-50 at 30°C and at pH 6.0 are shown in Figure 10. To compare the Langmuir isotherm and its ability to fit experimental data, the computed data for this isotherm are compared with experimental data for the adsorption of heavy metals (Fig. 10). It was found that for the adsorption of Pb(II), Hg(II), and Cd(II) on Ceralite, the Langmuir isotherm fits very well in the experimental data over the entire range of concentration. All the correlation coefficients for the Langmuir isotherm are more than 0.99. The maximum adsorption capacity Q^o and binding constant b for Ceralite IRC-50 calculated were found to be 189.80 mg g^{-1} and 0.014 L mg^{-1} for Hg(II), 123.67 mg g^{-1} and 0.017 L mg^{-1} for Pb(II), and 49.64 mg g^{-1} and 0.042 L mg^{-1} for Cd(II), respectively, which are considerably lower than those calculated for PGCP-COOH.

Test with industrial wastewater

Studies were conducted to find the suitability of the adsorbent for wastewater treatment. Simulated battery manufacturing industry wastewater with the composition[40] given in Table IV was used for Pb(II). Chlor-alkali industry wastewater sample for Hg(II)

TABLE IV
Composition of Wastewater Used for the Adsorption of Metals onto PGCP-COOH (mg L^{-1})

Pb(II) (Simulated battery manufacturing industry wastewater)
Pb^{2+}, 25.0; Ca^{2+}, 60.0; Na^+, 20.0; K^+, 5.0; Mg^{2+}, 15.0; Cl^-, 40.0; SO_4^{2-}, 170.0; NO_3^-, 40.0; SiO_2, 10.0.
Cd(II) (Fertilizer industry wastewater)
Cd^{2+}, 25.0; Hg^{2+}, 0.7; Na^+, 5.7; K^+, 10.9; Mg^{2+}, 0.1; Cl^-, 110.5; SO_4^{2-}, 65.0; NO_3^-, 1301.0; F^-, 10.4; CO_3^{2-}, 5.0; NH_3, 279.9; PO_4^{3-}, 6.3; BOD, 42.1; COD, 69.3; pH, 4.7; turbidity (NTU), 47.1; conductivity (mS cm^{-1}), 22.2.
Hg(II) (Chlor-alkali industry wastewater)
Hg^{2+}, 25.0; Pb^{2+}, 3.1; Cd^{2+}, 0.6; Mg^{2+}, 31.4; Ca^{2+}, 36.3; Na^+, 260.8; PO_4^{3-}, 13.1; NO_3^-, 17.1; NH_3, 27.1; Cl^-, 415.6; BOD, 61.5; COD, 165.1; pH, 8.3; turbidity (NTU), 41.6; conductivity (mS cm^{-1}), 19.1.

and fertilizer industry wastewater sample for Cd(II) were collected from local industries situated in the industrial belt of Cochin city (India). These wastewater samples were characterized by standard methods[41] and the compositions are given in Table IV. The concentration of Hg(II) and Cd(II) in the wastewater samples were found to be very low (2.86 mg L^{-1} for Hg(II) and 0.6 mg L^{-1} for Cd(II)) and so the samples were spiked with Hg(II) and Cd(II) solutions, so that the final metal concentration became 25 mg L^{-1}.

The effect of adsorbent dose on metal removal by PGCP-COOH was studied in all the cases. Figure 11 shows the effect of adsorbent dose on Pb(II), Hg(II), and Cd(II) removal from wastewaters. It was observed that for wastewater containing 25 mg L^{-1} of Pb(II) and Cd(II), an adsorbent dose of 100 and 140 mg, respectively, was required for complete removal. The chloralkali industry wastewater containing 25 mg L^{-1} of Hg(II) could be eliminated by 80 mg of adsorbent. These results are in good agreement with the batch experiments mentioned before. Consequently, the present study reveals that PGCP-COOH is an excellent adsorbent for Pb(II), Hg(II), and Cd(II) removal from wastewaters.

Reusability

For obtaining the reusability of the PGCP-COOH, the adsorption–desorption cycle was repeated three times with the same adsorbent and the results are shown in Table V. After three cycles the adsorption capacity of PGCP-COOH declined by 5.3, 6.9, and 8.5% for Hg(II), Pb(II), and Cd(II), respectively; whereas the desorption of metals in 0.2*M* HCl decreases from 95.2, 96.5, and 97.3% in the first cycle to 87.6, 89.0, and 91.3% in the third cycle. As seen here, resorption capacity of the PGCP-COOH for Pb(II), Hg(II), and Cd(II) ions is very high and did not significantly change during the repeated adsorption–desorption cycles. Desorption process can further clear up the mechanism of adsorption. If the adsorbed metal ions on PGCP-COOH surface can be desorbed easily by an acid solution, then the adsorption is competing with H^+. The desorption studies indicate that the mechanism governing the adsorption process cannot be ion exchange alone but may involve complexation through strong interaction between metals and PGCP-COOH.

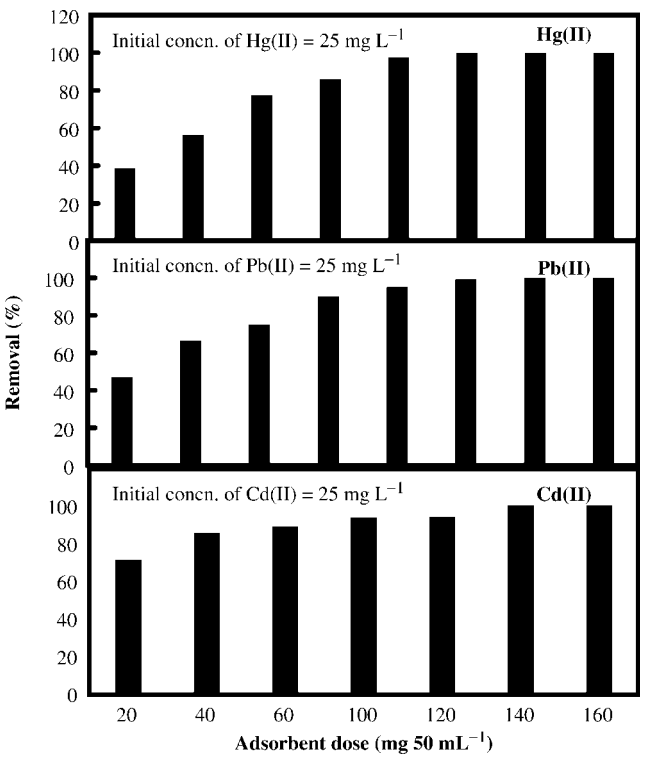

Figure 11 Effect of adsorbent dose for the removal of metals from wastewaters using PGCP-COOH.

TABLE V
Desorption and Regeneration Data

No. of cycles	Adsorption (%)	Desorption using 0.2*M* HCl (%)
Hg(II)		
1	99.7	95.2
2	97.0	91.0
3	94.4	87.6
Pb(II)		
1	95.8	96.5
2	91.2	94.2
3	88.9	89.0
Cd(II)		
1	99.7	97.3
2	96.2	93.6
3	91.2	91.3

CONCLUSIONS

In this study, a novel adsorbent (PGCP-COOH) carrying carboxylate functional group was prepared by grafting poly(AAm) onto CP using potassium peroxy sulphate as an initiator and in the presence of MBA as a crosslinking agent. The FTIR analysis showed the existence of carboxylate functional group with well-defined bands at 1762, 1267, and 3530 cm^{-1} frequencies. The adsorbent has a porous structure with a surface area of 42.3 m^2 g^{-1} and CEC of 1.87 meq g^{-1} and was effective for the removal of Pb(II), Hg(II), and Cd(II) ions from aqueous solutions. The removal capabilities of the PGCP-COOH were 2.8, 3.3, and 4.5 times of those of CP. Metal removal was efficiently performed in the initial pH range of 6.0–8.0, but efficiency decreased with a decrease of pH. The adsorption of Pb(II), Hg(II), and Cd(II) ions by PGCP-COOH reached equilibrium within 3 h and the adsorption followed a pseudo-second-order kinetics. This suggests that the rate-limiting step may be the chemisorption. The equilibrium isotherms of metal ions on the PGCP-

COOH were determined and successfully described by the Langmuir model. The adsorption capacities of the PGCP-COOH for Pb(II), Hg(II), and Cd(II) ions showed that it has sufficiently higher values compared with other adsorbents reported in the literature. The removal efficiency was tested using different industry wastewaters for Pb(II), Hg(II), and Cd(II) ions. The adsorbent was suitable for repeated use (for more than three cycles) without noticeable loss of capacity. Adsorption–desorption studies illustrate that PGCP-COOH could be used to remove Pb(II), Hg(II), and Cd(II) ions from aqueous solutions and other industrial effluents.

The authors are thankful to the Head, Department of Chemistry, University of Kerala, Trivandrum, for providing Laboratory facilities.

References

1. Ajmal, M.; Khan, A. H.; Ahmed, S.; Ahmed, A. Water Res 1998, 32, 3085.
2. Babel, S.; Kurniwan, T. A. J Hazard Mater B 2003, 97, 219.
3. Gupta, V. K.; Mohan, D.; Sharma, S.; Park, K. T. The Environmentalist 1999, 19, 129.
4. Ho, Y. S. Bioresour Technol 2005, 96, 1292.
5. Nada, A. M. A.; Eid, M. A.; Bahnasawy, R. M. E. C.; Khalifa, M. N. J Appl Polym Sci 2002, 85, 792.
6. Orlando, U. S.; Baes, A. U.; Nishijima, W.; Okada, M. Chemosphere 2002, 48, 1041.
7. Unnithan, M. R.; Vinod, V. P.; Anirudhan, T. S. J Appl Polym Sci 2002, 84, 2541.
8. Simkovic, I.; Laszlo, J. A. J Appl Polym Sci 1997, 64, 2561.
9. Unnithan, M. R.; Anirudhan, T. S. Ind Eng Chem Res 2001, 40, 2693.
10. Sreedhar, M. K.; Anirudhan, T. S. J Appl Polym Sci 2001, 25, 1261.
11. Miyajima, T. Water Res 2003, 37, 4945.
12. Noeline, B. F.; Manohar, D. M.; Anirudhan, T. S. Sep Purif Technol 2005, 45, 131.
13. Gopal, M.; Gupta, R. A. Ind Coconut J 2000, 31, 13.
14. Baes, A. U.; Okuda, T.; Nishijima, W.; Shoto, E.; Okada, M. Water Sci Technol 1997, 35, 39.
15. Unnithan, M. R.; Vinod, V. P.; Anirudhan, T. S. Ind Eng Chem Res 2004, 43, 2247.
16. Parab, H.; Joshi, S.; Shenoy, N.; Verma, R.; Lali, A.; Sudersanan, M. Bioresour Technol 2005, 96, 1241.
17. Schwarz, J. A.; Driscoll, C. T.; Bhanot, A. K. J Colloid Interface Sci 1984, 97, 55.
18. Maharana, S.; Tripathy, S. S. J Appl Polym Sci 1991, 42, 1001.
19. Shibi, I. G.; Anirudhan, T. S. J Chem Technol Biotechnol 2006, 81, 433.
20. Horowitz, H. H.; Metzger, G. Anal Chem 1963, 35, 1464.
21. Kim, J. H.; Lee, Y. M. Polymer 1993, 34, 1952.
22. Manju, G. N.; Krishnan, K. A.; Vinod, V. P.; Anirudhan, T. S. J Hazard Mater B 2002, 91, 221.
23. Shibi, I. G.; Anirudhan, T. S. Chemosphere 2005, 58, 1117.
24. Ho, Y. S.; McKay, G. Water Res 2000, 34, 736.
25. Aksu, Z.; Tezer, S. Process Biochem 2000, 36, 431.
26. Griffin, R. A.; Jurinak, J. J. Soil Sci Soc Am Proc 1973, 37, 369.
27. Giles, C. H.; McEwan, T. H.; Nakhwa, S. N.; Smith, D. J Chem Soc 1960, 4, 3973.
28. Selvaraj, K.; Chandramohan, V.; Pattabhi, S. J Sci Ind Res 1998, 57, 271.
29. Filho, N. L. D.; Polito, W. L.; Gushikem, Y. Talanta 1995, 42, 1031.
30. Manohar, M. D.; Anoop Krishnan, K.; Anirudhan, T. S. Water Res 2002, 36, 1609.
31. Namasivayam, C.; Periasamy, K. Water Res 1993, 27, 1663.
32. Balasubramanian, N.; Ahmed, A. J. Indian J Environ Prot 1997, 17, 601.
33. Ho, Y. S.; Huang, C. T.; Huang, H. W. Process Biochem 2002, 37, 1421.
34. Gupta, S. S.; Bhattacharya, K. G. Appl Clay Sci 2005, 30, 199.
35. Erdemoglu, M.; Erdemoglu, S.; Sayilkan, F.; Akarsu, M.; Sener, S.; Sayilkan, H. Appl Clay Sci 2004, 27, 41.
36. Malakul, A.; Srinivasan, K. R.; Wang, H. Y. Ind Eng Chem Res 1998, 37, 4296.
37. Namasivayam, C.; Ranganathan, K. Water Res 1995, 29, 1737.
38. Taty-Costodes, C. V.; Fauduet, H.; Porte, C.; Delacroix, A. J Hazard Mater B 2003, 105, 121.
39. Suzuki, Y.; Kametani, T.; Maruyama, T. Water Res 2005, 39, 1803.
40. Petruzzelli, D.; Pagano, M.; Tiravanti, G.; Passino, R. Solvent Extr Ion Exch 1994, 17, 667.
41. APHA. Standard Methods for the Examination of Water and Wastewater, 18th ed.; APHA, AWWA, and WEF: Washington, DC, 1992.